Journal of Marine Science and Engineering

MDPI

Article

Optimization of Process Parameters in Friction Stir Welding of Aluminum 5451 in Marine Applications

Shoaib Ahmed [1], Rana Atta ur Rahman [1], Awais Awan [2], Sajjad Ahmad [3,*], Waseem Akram [3], Muhammad Amjad [3], Mohd Yazid Yahya [4] and Seyed Saeid Rahimian Koloor [4,5,6,*]

[1] Department of Mechanical Engineering, University of Engineering and Technology, Taxila 47050, Pakistan
[2] Department of Mechanical Engineering, Quaid-e-Azam College of Engineering & Technology, Sahiwal 57000, Pakistan
[3] Department of Mechanical Engineering, International Islamic University Islamabad, Islamabad 44000, Pakistan
[4] Centre for Advanced Composite Materials, School of Mechanical Engineering, Faculty of Engineering, Universiti Teknologi Malaysia, Bahru 81310, Malaysia
[5] Institute for Nanomaterials, Advanced Technologies and Innovation (CXI), Technical University of Liberec (TUL), Studentská 1402/2, 461 17 Liberec, Czech Republic
[6] Institute for Structural Engineering, Department of Civil Engineering and Environmental Sciences, Universität der Bundeswehr München, Werner-Heisenberg-Weg 39, Neubiberg, 85579 Munich, Germany
* Correspondence: sa.ahmad@iiu.edu.pk (S.A.); seyed.rahimian@unibw.de (S.S.R.K.)

Abstract: Friction stir welding (FSW) is one of the primary fabrication techniques for joining different components, and it has become popular, especially in aluminum alloy structures for marine applications. The welded joint with the friction stir process greatly depends on the process parameters, i.e., feed rate, rotational speed, and pin profile of the tool. In the current study, plates of aluminum 5451 alloy were joined by the FSW technique, and the Taguchi method was used to find the process parameters at an optimal level. The maximum value of tensile strength, i.e., 160.6907 MPa, was achieved using optimum welding conditions of a tool rotation speed of 1400, a feed rate of 18 mm/min, and the tool pin with threads. The maximum value of hardness, i.e., 81.056 HV, was achieved using optimum conditions of 1200 tool rotational speed and a feed rate of 18 mm/min with a tool pin profile having threads. In addition, the contribution in terms of the percentage of each input parameter was found by the analysis of variance (ANOVA). The ANOVA results revealed that the pin profile of the tool has the maximum contribution of 67.77% and 62.42% in achieving the optimum value of tensile strength and hardness, respectively. The study also investigated the joint efficiency of the friction stir welded joint, hardness at the weld zone, and metallography on FSW samples at the optimized level. The effectiveness and reliability of FSW joints for shipping industry applications can be observed by joint efficiency. That was investigated at optimum conditions, and it comes out to be 80.5%.

Keywords: aluminum alloy 5451; friction stir welding; Taguchi method; analysis of variance; optimization

Citation: Ahmed, S.; Rahman, R.A.u.; Awan, A.; Ahmad, S.; Akram, W.; Amjad, M.; Yahya, M.Y.; Rahimian Koloor, S.S. Optimization of Process Parameters in Friction Stir Welding of Aluminum 5451 in Marine Applications. *J. Mar. Sci. Eng.* **2022**, *10*, 1539. https://doi.org/10.3390/jmse10101539

Academic Editors: K. Reza Kashyzadeh and Mahmoud Chizari

Received: 25 September 2022
Accepted: 14 October 2022
Published: 19 October 2022

1. Introduction

Aluminum and its alloys are frequently utilized in the design of complex marine construction such as hulls and deck panels of ships [1–3], as well as in other advanced industries such as automotive, defense, and aerospace [4–6]. This is due to aluminum's outstanding mechanical properties, such as its high strength-to-weight ratio, low density, high resistance to corrosion, easy fabrication, and recycling [7,8]. Marine-grade aluminum alloys are known to be corrosion-resistant under seawater, making them ideal to be use

in marine applications [9]. It is also broadly used in the manufacturing of hybrid aluminum composite structures to improve the applicability and durability of the structures for harsh environmental and operational conditions [10–12]. However, aluminum alloys to be used in complex geometry for joint applications faced several challenges including conventional welding methods. Conventional welding includes fusion welding, which is further categorized as electric welding and gas welding [13]. For example, one of the main disadvantages of fusion welding [14] is a complete alteration of microstructure and inferior mechanical properties. In fusion welding, the temperature at the weld zone is high, due to which cracking occurs in the welded region. One of the methods to reduce the cracking is to reduce the input heat, which is possible in laser beam welding or a solid-state joining method such as friction stir welding. The issues such as cracking, recrystallization of the grain, and porosity can be prevented in friction stir welding (FSW), which provides improved joint properties compared to fusion weld joints [15,16]. Friction stir welding (FSW) is a well-known solid-state joining technique in which a non-consumable rotating tool is used to join two facing workpieces without melting the workpiece material.

The FSW technique can be applied to weld similar and dissimilar metals and is gaining popularity nowadays [17]. During the FSW process, a non-consumable welding tool is forcibly plunged into the joint line of plates to be welded with a particular rotation speed. The tool travels along the length of the joint and creates sufficient heat through friction to plastically deform the material [18]. The weld zone in the FSW consists of the heat-affected zone (HAZ), thermos-mechanically affected zone (TMAZ), and the nugget zone (so-called stir zone (ST)). In the HAZ, no plastic deformation occurs in the materials; however, the welding heat affects this region and causes some microstructural changes. In the second zone, i.e., TMAZ, the generated heat during the FSW affects the material and becomes partially deformed. Finally, the material is deformed severely in the SZ at the pin location during the welding [18].

Joints made with FSW are much stronger and more economical than traditional fusion welding techniques [19–21]. Furthermore, FSW improves weld quality, reduces defects, and lowers health hazards [22]. The most significant parameters that contribute to the weld quality and affect the welded zone properties include the tool pin profile, rotation speed of the tool, and feed rate [23].

In previous research, Gomathisankar et al. [24] investigated FSW parameters using the Taguchi method on AA-6061 to examine the friction stir welded region's mechanical properties. The result revealed that the feed rate played an essential role in improving tensile strength and hardness. In comparison, the tool rotation speed, time of dwell, and tilt angle of the tool have comparatively less effect on mechanical properties. Dawood et al. [25] considered AA6061 to study the influence of pin profiles of the tool on the friction stir welded joints' mechanical properties. The fracture surface analysis indicated that the joints were affected using different pin profiles of the tool. Shojaeefard et al. [26] optimized the tool rotation speed, feed rate, and tool shoulder diameter for tensile strength, grain size, and hardness using Taguchi's technique. The optimum conditions were an 1120 tool rotational speed, a 1.5-degree tilt angle, and a 6.5 mm/min feed rate. The maximum hardness value occurred in the middle of the welded nugget region (ST) because of the formation of tiny, recrystallized grains. Boldsaikhan et al. [27] introduced a new technique for the detection of wormhole defects in the FSW in a non-destructive manner. They demonstrated an approach that provided feedback information for weld quality in real time. Baratzadeh et al. [18] studied the mechanical properties and microstructure of the FSW joint of automotive aluminum alloys AA-6082-T6 and AA-6063-T6. Their study identified the enhanced process parameters using dissimilar aluminum alloys for increased weld quality. Msomi et al. [28] discussed the joint quality of 5083-H111 and 1050-H14 aluminum alloys joined by friction stir welding. The microstructure and mechanical properties of the welded joint were analyzed and compared with base materials. The correlation between the mechanical behavior and microstructure of the welded joint was discussed.

The results indicated that the tensile strength of the welded joint was larger than the AA-1050-H14 and lower than AA-5083-H111. The micro-hardness of the friction stir region was greater than AA-1050-H14 and came in the same range when compared with AA-5083-H111. Recently, Nakowong and Sillapasa [29] used the Taguchi method, regression analysis and analysis of variance for the optimization of process parameters for the FSW. Their focus was tensile strength, hardness, and microstructure; however, the studied material was the semi-solid metal 5083 aluminum alloy.

This manuscript addresses the optimization of welding process parameters in Friction Stir Welding (FSW) for a commercial aluminum alloy. The above-mentioned literature review shows that such a study is very important for large structural design and industrial decision-making. To the best of the authors' knowledge, although few studies investigate the process parameters of some materials in the joint process, however, there are no studies that optimize the process parameters of FSW on aluminum alloy 5451, which is frequently used in many industrial applications, including marine applications due to its excellent weldability and corrosion resistance.

In this regard, the current work uses the Taguchi method to optimize the FSW process parameters of aluminum alloy 5451 considering the process parameters of tool rotational speed and feed rate on three different tool geometries. The focus of the study is to analyze the tensile strength and hardness at the weld zone; however, the joint efficiency and microstructure at the weld zone are also examined. Additionally, the analysis of variance (ANOVA) was applied to calculate the percentage contributions of input parameters in improving the tensile strength and hardness of the weld.

2. Materials and Methods

Commercially available AA5451 was used in the present study. The dimensions of AA5451 plates were 900 mm × 60 mm × 6 mm. The chemical composition of the AA5451 was found using spectromax, and the obtained results are shown in Table 1.

Table 1. Chemical composition of AA-5451.

Al	Si	Mg	Fe	Cr	Mn	Cu	V	Ti	Zn	P
97.19%	0.07%	2.23%	0.17%	0.2%	0.08%	0.004%	0.02%	0.02%	0.01%	0.002%

A vertical head CNC milling machine was used to prepare sheared face edges with excellent finishing and perpendicularity. Three pairs of plates were welded with three different regions having varying parameters for process optimization. These factors with their levels are given in Table 2. The welding direction and rolling direction were perpendicular to each other, and a single weld pass was used to fabricate the joints. The same tools were previously recommended by Nakowong and Sillapasa [29]; however, their base material was Al5083. In addition, they used the tool pin profile with different levels of tool rotational speed. Furthermore, their levels of feed rates were different from those selected in this study. The selected tool was made of HSS (H-13) material with three geometries, as presented in Figure 1.

Table 2. Input parameters are involved along with their levels.

Factors	Level 1	Level 2	Level 3
Tool Rotation Speed (rpm)	1000	1200	1400
Feed Rate (mm/min)	16	18	20
Tool Pin Profile	Taper	Threaded	Cylindrical

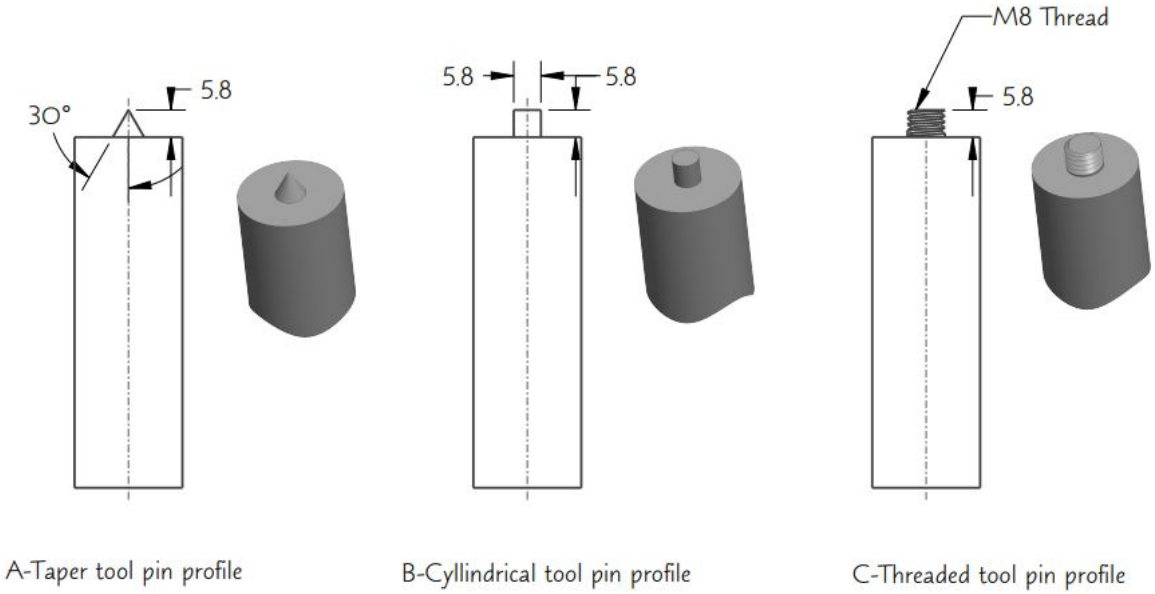

Figure 1. Tool profiles in the FSW process.

ASTM E8 [30] standard was applied for the preparation of tensile test specimens, as depicted in Figure 2. It was ensured that the gauge length of the tensile specimens incorporates the central part of the welded region. A strain rate of 3 mm/min was set up until the complete fracture of specimens. Finally, the ultimate tensile strength was obtained from the stress-strain curve for each specimen welded with different process parameters. Figure 3A,B shows the tensile specimen before the test and after failure.

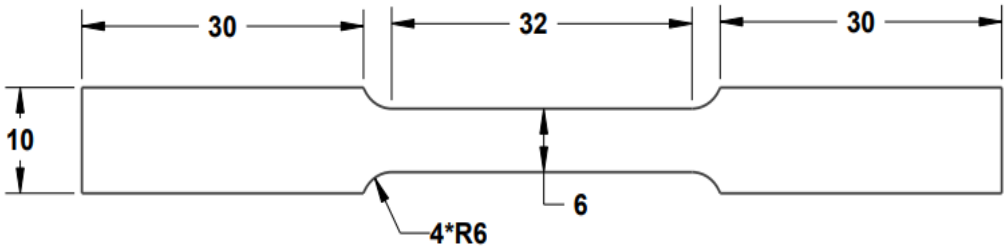

Figure 2. The geometry of tensile test specimens is based on the standard.

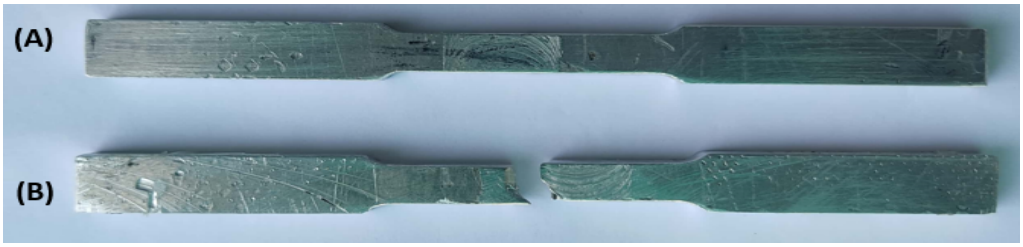

Figure 3. Samples used in the tensile test; (**A**) before and (**B**) after the test.

Furthermore, the microhardness values were taken at the bead. The microhardness test on the friction stir welded region was performed using ASTM E92 on a low load Vickers tester (HV-5 Digital Vickers Hardness Tester) with 10 to 20 s dwelling time. The distance between two consecutive dents is kept according to the standard, i.e., 2.5 times the mean value of the diagonal of indentation. For the optimization of parameters, the Taguchi method was implemented that includes an L_9 orthogonal array using all three factors with their respective levels. Therefore, welding was carried out for nine different combinations based on the input parameters given in Table 3.

Table 3. Input variables or L_9 orthogonal array.

Sr. No	Tool Rotation Speed (rpm)	Feed Rate (mm/min)	Tool Pin Profile
1	1000	16	Taper
2	1000	18	Threaded
3	1000	20	Cylindrical
4	1200	16	Threaded
5	1200	18	Cylindrical
6	1200	20	Taper
7	1400	16	Cylindrical
8	1400	18	Taper
9	1400	20	Threaded

The study is organized around optimizing the process parameters to achieve higher tensile strength and hardness values. However, the other output parameters, such as joint efficiency, and metallography on FSW samples, were also performed. This investigation was carried out using the process parameters at the optimum level obtained after the tensile test and the hardness of FSW joints. For metallography, the specimens were prepared as per ASTM E3-01 standard, and microscopic investigations were carried out using a Zeiss Axiovert 100 A microscope (magnification 25×~1000×). Finally, the percentage contribution of each parameter was found by analysis of variance. A 95% confidence interval is taken while performing an analysis of variance, which is usually used by researchers [31,32].

3. Results and Discussion

3.1. Process Parameters Optimization for the Tensile Strength and Hardness

In this study, the Taguchi method was used to optimize process parameters to obtain a higher value of tensile strength and hardness of AA5451 after FSW. In the Taguchi method, experimental values are converted into signal-to-noise ratios. The larger the better signal-to-noise ratio (S/N ratio) criteria were chosen to maximize the response using Equation (1) [33]. Experimental results, along with signal-to-noise ratios, are shown in Table 4.

$$\text{S/N ratio } (\eta) = -10 \log_{10} \frac{1}{n} \sum_{i=1}^{n} \frac{1}{y_i^2} \quad (1)$$

where n = number of experiments, $y_i = i^{th}$ experimental value for the parameter

Table 4. Result of experiments and corresponding signal-to-noise ratios.

Trial No	Orthogonal Array with Control Factors			Experimental Layout with Control Factors and Levels			Experimental Results		S/N Ratios	
	Tool Rotational Speed	Feed Rate	Tool Pin Profile	Tool Rotational Speed	Feed Rate	Pin Profile of Tool	Tensile Strength (Mpa)	Hardness (Weld Zone)	Tensile strength (Mpa)	Hardness (Weld Zone)
1	1	1	1	1000	16	Taper	110.91	69.5	40.8996	36.8397
2	1	2	2	1000	18	Threaded	150.60	79.6	43.5565	38.0183
3	1	3	3	1000	20	Cylindrical	120.20	72.1	41.5981	37.1587
4	2	1	2	1200	16	Threaded	155.80	78.2	43.8513	37.8641
5	2	2	3	1200	18	Cylindrical	127.60	77.3	42.1170	37.7636
6	2	3	1	1200	20	Taper	118.90	70.7	41.5036	36.9884
7	3	1	3	1400	16	Cylindrical	139.00	73.5	42.8603	37.3257
8	3	2	1	1400	18	Taper	136.70	73.7	42.7154	37.3493

9	3	3	2	1400	20	Threaded	143.66	74.9	43.1467	37.4896

The main effect plots from Figure 4 and S/N ratios from Table 5 show that the optimum conditions for high tensile strength are a 1400 tool rotational speed, a feed rate of 18 mm/min, and a threaded tool pin profile. Figure 5 and Table 5 also show that the optimum conditions at which hardness values are obtained are the tool rotational speed of 1200, feed rate of 18 mm/min, and the threaded tool pin profile. A likely explanation for this is that the threaded pin profile made a flawless joint due to the adequate stirring of material around the pin. It is also evident from previous research that the tool shoulder generates 80%, and the tool pin profile produces 20% of total heat generation during stirring [34]. However, the influence of the tool pin profile on material flow behavior is more significant than the tool shoulder [35].

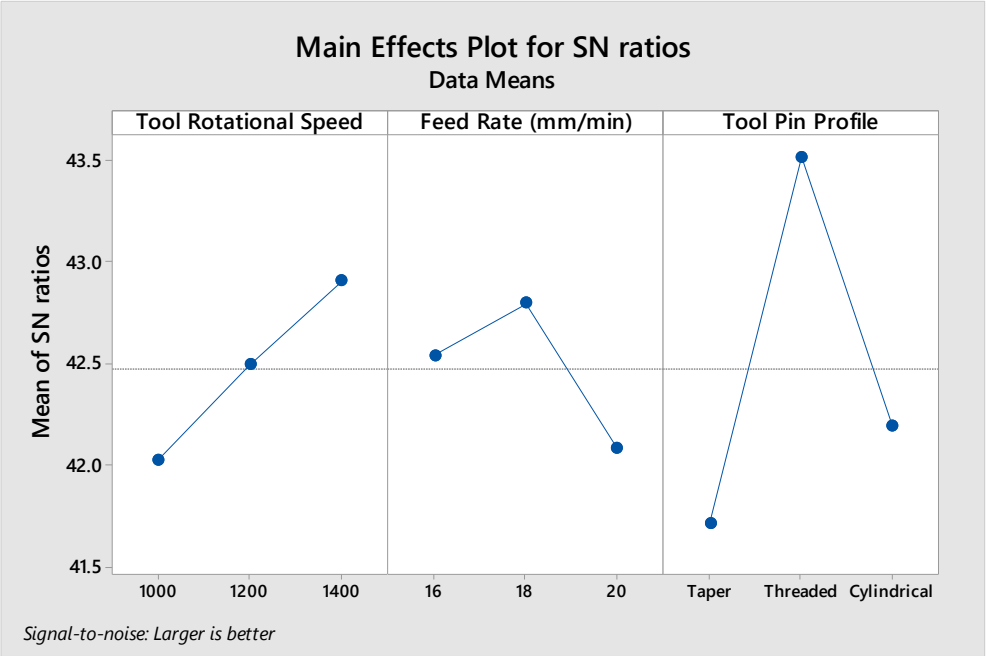

Figure 4. Main effect plot of signal-to-noise ratio for tensile strength.

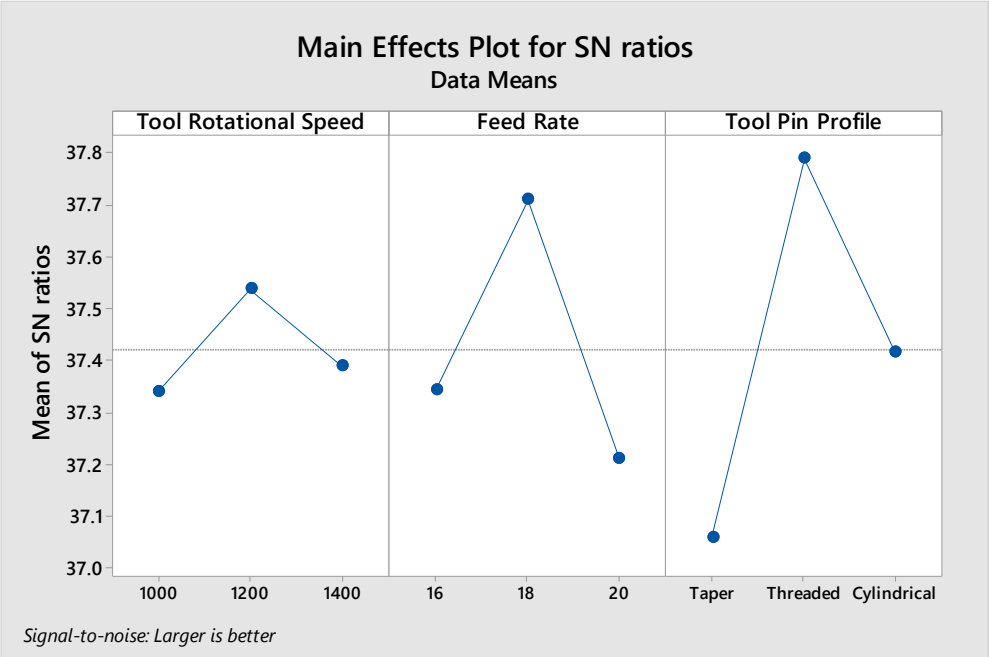

Figure 5. Main effect plot of signal-to-noise ratio for hardness (weld zone).

Table 5. Tensile strength and hardness S/N ratios.

S/N Ratio Response Values for Tensile Strength			
Level	**Tool Rotational Speed(rpm)**	**Feed Rate (mm/min)**	**Tool Pin Profile**
1	42.02	42.54	41.71
2	42.49	**42.80** [a]	**43.52** [a]
3	**42.91** [a]	42.08	42.19
Delta	0.89	0.71	1.81
Rank	2	3	1

S/N Ratio Response Values for Hardness			
Level	**Tool Rotational Speed(rpm)**	**Feed Rate (mm/min)**	**Tool Pin Profile**
1	37.34	37.34	37.06
2	**37.54** [a]	**37.71** [a]	**37.79** [a]
3	37.39	37.21	37.42
Delta	0.20	0.5	0.73
Rank	3	2	1

[a] Optimum value.

3.2. Results Using Analysis of Variance

Analysis of variance is used to understand the effect of each input parameter on the output parameters. The input parameters used in the current study are feed rate, tool rotational speed, and tool pin profile, while the responses in this study are tensile strength and hardness. The confidence interval taken into consideration for the current investigation was 95%. Table 6 displays the input parameters' contributions in terms of the percentage of responses. Table 6 shows that the tool rotation speed has an impact of 12.68%, the feed rate speed has an impact of 9.78%, and the tool pin profile has an effect of 67.77% on the tensile strength. Therefore, the pin profile of the tool has more impact than the feed rate and rotational speed of the tool on the tensile strength. Koilraj et al. [36] investigated the optimum parameters for friction stir welding between two dissimilar alloys (Al-Mg alloy AA5083-H3219 and Al–Cu alloy AA2219-T87) by Taguchi's method. Four different pin profiles of the tool used were used, i.e., cylindrical, tapered cylindrical, tapered threaded, and cylindrically threaded, and it was concluded that the threaded pin profile of the tool gave the best results in terms of tensile strength. However, in this study, the confidence interval taken was 95%. Therefore, those parameters become insignificant, whose p-value is greater than 0.05. Thus, none of the parameters is significant at a 95% confidence level. For hardness, the tool rotational speed has an impact of 5.01%, a feed rate of 31.42%, and a pin profile of the tool of 62.42%. The hardness pin profile of the tool and feed rate are significant parameters, while the rotational speed of the tool becomes insignificant. Table 4 also revealed that the significant process parameters affecting the hardness at a 95% confidence level were tool pin profiles following the feed rate and rotational speed, which is in agreement with previous studies [31].

Table 6. ANOVA table for tensile strength and hardness.

Source	D.F	Seq. SS	Contribution	Adj. SS	Adj. MS	F-Value	P-Value
Tensile Strength							
Tool Rotation Speed	2	236.9	12.68%	236.9	118.46	1.30	0.435
Feed Rate	2	182.7	9.78%	182.7	91.34	1.00	0.500
Pin Profile of Tool	2	1266.0	67.77%	1266.0	632.98	6.94	0.126

Error	2	182.5	9.77%	182.5	91.26	-	-
Total	8	1868.1	100.00%	-	-	-	-
Hardness (Weld Zone)							
Tool Rotation Speed	2	4.74	5.01%	4.74	2.368	4.38	0.186
Feed Rate	2	29.67	31.42%	29.67	14.834	27.41	0.035
Pin Profile of Tool	2	58.94	62.42%	58.94	29.471	54.46	0.018
Error	2	1.08	1.15%	1.08	0.541	-	-
Total	8	94.43	100%	-	-	-	-

3.3. Response Optimization for Tensile Strength and Hardness

Response optimization identifies the combination of input variables that collectively optimize single or multiple output responses. The input parameters are the Tool Rotational Speed, Feed Rate, and Tool Pin with the combination shown in Table 4. The output response is the tensile strength. The tensile strength value predicted by the response optimization technique was 160.6907 Mpa obtained at an 18 mm/min feed rate and 1400 rotational speed with the threaded tool pin profile, as given in Table 7.

Table 7. Response optimization for tensile strength.

Parameters						
Response	**Goal**	**Lower**	**Target**	**Upper**	**Weight**	**Importance**
Tensile strength (Mpa)	Maximum	110.912	155.8	-	1	1
Solution						
Solution	Tool rotational speed	Feed rate	Tool pin profile	Tensile strength (Mpa) fit		Composite desirability
1	1400	18	Threaded	**160.691**		1
Multiple Response Prediction						
Variable				Setting		
Tool rotation speed				1400		
Feed rate				18		
Pin profile of the tool				Threaded		
Response		Fit	SE Fit	95% CI	95% PI	
Tensile strength (Mpa)		**160.69**	8.43	(124.44, 196.94)	(105.88, 215.50)	

Similarly, the hardness value of 81.056 HV was predicted with a feed rate of 18 mm/min, the tool rotation speed of 1200 rpm, and the threaded pin profile of the tool, as given in Table 8.

Table 8. Response optimization for hardness.

Parameters						
Response	**Goal**	**Lower**	**Target**	**Upper**	**Weight**	**Importance**
Hardness (Hv)	Maximum	69.5	79.6		1	1
Solution						
Solution	Tool rotational speed	Feed rate	Tool Pin profile	Hardness (Hv) Fit		Composite Desirability
1	1200	18	Threaded	**81.0556**		1
Multiple Response Prediction						
Variable				Setting		
Tool Rotation Speed				1200		
Feed rate				18		

Pin Profile of tool			Threaded	
Response	Fit	SE Fit	95% CI	95% PI
Hardness (Hv)	**81.056**	0.649	(78.264, 83.847)	(76.835, 85.276)

3.4. Joint Efficiency at Optimum Level

From the response optimizer data, the optimum parameters considered for tensile strength were a 1400 tool rotational speed, an 18 mm/min feed rate, and a threaded pin profile. Therefore, the tensile strength value at the optimal level of the welded specimen was found as 157 Mpa, thus validating the optimum combination of parameters. Additionally, the experimental tensile strength of the base material AA5451 was found as 195 Mpa. Therefore, the joint efficiency at optimum conditions comes out to be 80.5% calculated using Equation (2).

$$\text{Joint Efficiency} = \frac{\text{Strength of weld}}{\text{Strength of base material}} \quad (2)$$

3.5. Hardness Properties at Optimum Level

The microhardness test on the friction stir welded region was performed using an ASTM E92 on a low-load Vickers tester (HV-5 Digital Vickers Hardness Tester) with 10 to 20 s dwelling time. The distance between two consecutive dents is kept according to the standard, i.e., 2.5 times the mean value of the diagonal of indentation. For the samples welded under optimum process parameters, i.e., a tool rotational speed of 1200, a feed rate of 18 mm/min, and a threaded pin profile, the Vickers hardness values at different regions were measured, as shown in Figure 6. These regions include the advancing side, bead, HAZ, and retarding side. The hardness of the advancing side and retarding side was found to be the same and lower from the bead. However, the friction stir welded region exhibits a higher value of Vickers microhardness than the base region, which could be expected from the refined grain size. Since the microstructure of the advancing side and retarding side are not affected by the welding process, their values are comparatively lower and different from those of the weld zone.

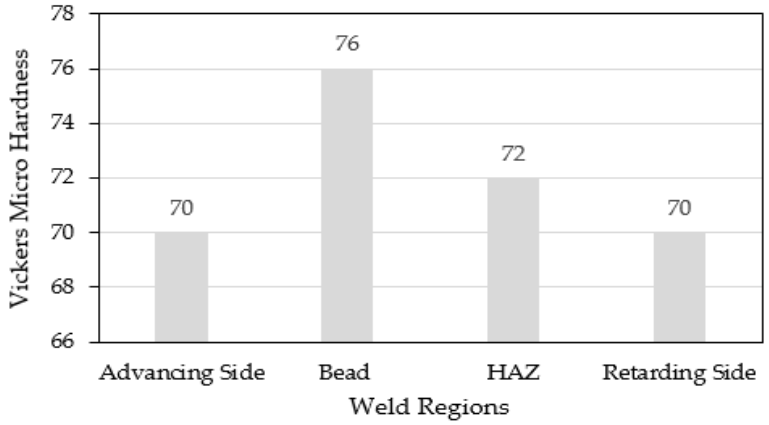

Figure 6. Vickers microhardness of the weld regions.

3.6. Microstructures at Optimum Level

For microscopic tests, a specimen is prepared according to the ASTM E3-01 standard. The test is performed on a Zeiss Axiovert 100 A. The microstructure of the samples made at the optimum levels described in Section 3.5 was analyzed and matched with the base metal as presented in Figure 7. In the base region of AA5451, the grain size is larger.

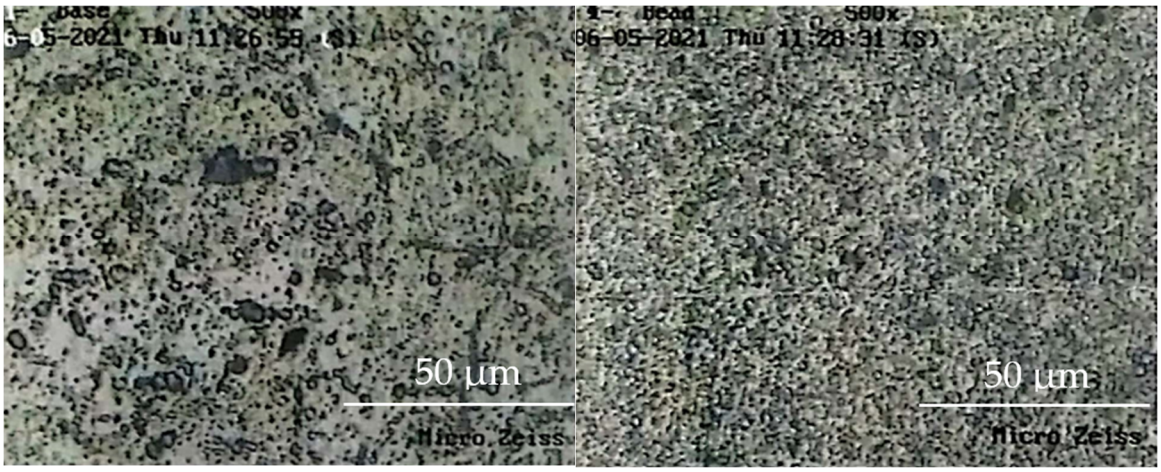

Figure 7. Optical micrographs of AA5451(base metal) and FSW region at an optimum level.

In contrast, the friction stir welded region has smaller grains. This result indicates that the friction stir welded region is deformed plastically due to the spinning probe's mechanical stirring action. After the stirring action, the grains are modified by dynamic recrystallization. Recrystallization of the grains into the fine structure is also observed in the research work reported by Hall-Petch [37]. A refinement of grain size was observed in this study with an increased value of the tool rotational speed. This improved microstructure would lead to welded joints with enhanced mechanical properties [38].

4. Conclusions

This study addresses the FSW technique for aluminum 5451 component joints in the structural application of marine and other advanced industries. The optimum level of the process parameters in FSW was found by the Taguchi method, and ANOVA was used to evaluate the percentage contribution of each factor. The following results were concluded from the present study.

- The highest value of tensile strength, i.e., 160.6907 Mpa, was calculated on the optimizer plot with optimum conditions of a 1400 tool rotation speed, a feed rate of 18 mm/min, and the tool pin with threads.
- The tensile strength of 157 Mpa was found experimentally for the specimen prepared using the optimum conditions, thus validating the computed results.
- The improved tensile strength was attributed to grain size refinement, which is directly related to the high rotational speed of the tool, sufficient feed rate, and geometry of the tool pin profile that provides better stirring action in the weld zone.
- The maximum value of hardness, i.e., 81.056 HV, was shown by friction stir welded joints fabricated using optimum conditions of a 1200 tool rotational speed, a feed rate of 18 mm/min, and a threaded tool pin profile.
- The higher value of Vickers microhardness was also observed in the friction stir zone due to the refining microstructure.
- Tool geometry was the major factor affecting tensile strength, contributing 67.77%, while feed rate has the least effect on tensile strength, contributing 9.78%.
- Tool geometry was the major factor affecting the hardness, contributing 62.42%, while tool rotation speed has the least effect on hardness, contributing 5%.
- The effectiveness and reliability of FSW joints for shipping industry applications can be observed by joint efficiency. That was investigated at optimum conditions, and it comes out to be 80.5%.

Author Contributions: Conceptualization, S.A. (Shoaib Ahmed), and R.A.u.R.; methodology, S.A. (Shoaib Ahmed), R.A.u.R. and S.A. (Sajjad Ahmad); software, S.A. (Shoaib Ahmed), A.A.; validation, S.A. (Shoaib Ahmed), R.A.u.R., A.A., S.A. (Sajjad Ahmad), W.A., M.A., M.Y.Y., S.S.R.K.; formal analysis, S.A. (Shoaib Ahmed), S.A. (Sajjad Ahmad), S.S.R.K. and M.Y.Y.; investigation, S.A. (Shoaib Ahmed); resources, S.A. (Sajjad Ahmad) and S.S.R.K.; data curation, M.A.; writing—original draft preparation, S.A. (Shoaib Ahmed), and R.A.u.R.; writing—review and editing, S.A. (Shoaib Ahmed), R.A.u.R., A.A., S.A. (Sajjad Ahmad), W.A., M.A., M.Y.Y., S.S.R.K.; visualization, W.A., M.A., and S.A. (Sajjad Ahmad); supervision, R.A.u.R.; project administration, S.S.R.K., and R.A.u.R.; funding acquisition, S.S.R.K. All authors have read and agreed to the published version of the manuscript.

Funding: The authors acknowledge the support of Universiti Teknologi Malaysia through project No. Q.J130000.21A6.00P39.

Institutional Review Board Statement: Not applicable.

Informed Consent Statement: Not applicable.

Acknowledgment: The authors acknowledge the support of Universiti Teknologi Malaysia through project No. Q.J130000.21A6.00P39, as well as the support from the Minister of Transport and Construction of the Slovak Republic and the European Union in the transport sector and Information Technology in the frames of the project "Adaptation of 21st century technologies for non-conventional low-emission vehicles based on composite materials ", Reg. No. NFP313010BXF3 by OPII–VA/DP/2021/9.3-01.

Conflicts of Interest: There is no conflict to declare.

References

1. Wahid, M.A.; Siddiquee, A.N.; Khan, Z.A. Aluminum alloys in marine construction: Characteristics, application, and problems from a fabrication viewpoint. *Mar. Syst. Ocean Technol.* **2020**, *15*, 70–80.
2. Hosseinabadi, O.F.; Khedmati, M.R. A review on ultimate strength of aluminium structural elements and systems for marine applications. *Ocean Eng.* **2021**, *232*, 109153.
3. Martin, J.; Wei, S. Friction stir welding technology for marine applications. In *Friction Stir Welding and Processing VIII*; Springer: Berlin/Heidelberg, Germany, 2015; pp. 219–226.
4. Starke Jr, E.A.; Staley, J.T. Application of modern aluminum alloys to aircraft. *Prog. Aerosp. Sci.* **1996**, *32*, 131–172.
5. Abdi, B.; Koloor, S.; Abdullah, M.; Amran, A.; Yahya, M.Y. Effect of strain-rate on flexural behavior of composite sandwich panel. *Appl. Mech. Mater.* 2012, 229, 766–770.
6. Shah, I.A.; Khan, R.; Koloor, S.S.R.; Petrů, M.; Badshah, S.; Ahmad, S.; Amjad, M. Finite Element Analysis of the Ballistic Impact on Auxetic Sandwich Composite Human Body Armor. *Materials* **2022**, *15*, 2064.
7. Shokravi, H.; Mohammadyan-Yasouj, S.E.; Koloor, S.S.R.; Petrů, M.; Heidarrezaei, M. Effect of alumina additives on mechanical and fresh properties of self-compacting concrete: A review. *Processes* **2021**, *9*, 554.
8. Mazlan, S.; Yidris, N.; Koloor, S.S.R.; Petrů, M. Experimental and Numerical Analysis of Fatigue Life of Aluminum Al 2024-T351 at Elevated Temperature. *Metals* **2020**, *10*, 1581.
9. Kishta, E.E.; Darras, B. Experimental investigation of underwater friction-stir welding of 5083 marine-grade aluminum alloy. *Proc. Inst. Mech. Eng. Part B J. Eng. Manuf.* **2016**, *230*, 458–465.
10. Nia, A.B.; Nejad, A.F.; Xin, L.; Ayob, A.; Yahya, M.Y.; Koloor, S.S.R.; Petrů, M.; Hassan, S.A. Dynamic response of aluminium sheet 2024-T3 subjected to close-range shock wave: Experimental and numerical studies. *J. Mater. Res. Technol.* **2021**, *10*, 349–362.
11. Chow, Z.P.; Ahmad, Z.; Wong, K.J.; Koloor, S.S.R.; Petrů, M. Thermal Delamination Modelling and Evaluation of Aluminium–Glass Fibre-Reinforced Polymer Hybrid. *Polymers* **2021**, *13*, 492.
12. Kashyzadeh, K.R.; Rahimian Koloor, S.S.; Omidi Bidgoli, M.; Petrů, M.; Amiri Asfarjani, A. An optimum fatigue design of polymer composite compressed natural gas tank using hybrid finite element-response surface methods. *Polymers* **2021**, *13*, 483.
13. Praveen, P.; Yarlagadda, P. Meeting challenges in welding of aluminum alloys through pulse gas metal arc welding. *J. Mater. Processing Technol.* **2005**, *164*, 1106–1112.
14. Cheng, Y.; Hu, Y.; Xu, J.; Yu, L.; Huang, T.; Zhang, H. Studies on Microstructure and Properties of TiB2-Al3Ti Ceramic Particles Reinforced Spray-Formed 7055 Aluminum Alloy Fusion Welded Joints. *J. Mater. Res. Technol.* **2022**.
15. Morozova, I.; Królicka, A.; Obrosov, A.; Yang, Y.; Doynov, N.; Weiß, S.; Michailov, V. Precipitation phenomena in impulse friction stir welded 2024 aluminium alloy. *Mater. Sci. Eng. A* **2022**, *852*, 143617.
16. Arunprasad, R.; Surendhiran, G.; Ragul, M.; Soundarrajan, T.; Moutheepan, S.; Boopathi, S. Review on friction stir welding process. *Int. J. Appl. Eng. Res. ISSN* **2018**, *13*, 5750–5758.

17. Chauhan, A.; Kumar, S. Impact strength of joints of aluminium matrix composite formed using friction stir welding technique. *Mater. Today Proc.* **2021**, *38*, 234–236.
18. Baratzadeh, F.; Boldsaikhan, E.; Nair, R.; Burford, D.; Lankarani, H. Investigation of mechanical properties of AA6082-T6/AA6063-T6 friction stir lap welds. *J. Adv. Join. Process.* **2020**, *1*, 100011.
19. Cabibbo, M. Friction Stir Welding Prospective on Light-Alloys Joints. *Metals* 2022, 12, 560.
20. Nguyen, T.V.; Huynh, N.-T.; Vu, N.-C.; Kieu, V.N.; Huang, S.-C. Optimizing compliant gripper mechanism design by employing an effective bi-algorithm: Fuzzy logic and ANFIS. *Microsyst. Technol.* **2021**, *27*, 3389–3412.
21. Wang, C.-N.; Yang, F.-C.; Nguyen, V.T.T.; Nguyen, Q.M.; Huynh, N.T.; Huynh, T.T. Optimal Design for Compliant Mechanism Flexure Hinges: Bridge-Type. *Micromachines* **2021**, *12*, 1304.
22. Boldsaikhan, E.; McCoy, M. Analysis of tool feedback forces and material flow during friction stir welding. In *Friction Stir Welding and Processing VII*; Springer: Berlin/Heidelberg, Germany, 2013; pp. 311–320.
23. Venkateswarlu, D.; Mandal, N.; Mahapatra, M.; Harsh, S. Tool design effects for FSW of AA7039. *Weld. J.* **2013**, *92*, 41–47.
24. Gomathisankar, M.; Gangatharan, M.; Pitchipoo, P. A novel optimization of friction stir welding process parameters on aluminum alloy 6061-T6. *Mater. Today Proc.* **2018**, *5*, 14397–14404.
25. Dawood, H.; Mohammed, K.S.; Rahmat, A.; Uday, M. Effect of small tool pin profiles on microstructures and mechanical properties of 6061 aluminum alloy by friction stir welding. *Trans. Nonferrous Met. Soc. China* **2015**, *25*, 2856–2865.
26. Shojaeefard, M.H.; Khalkhali, A.; Akbari, M.; Tahani, M. Application of Taguchi optimization technique in determining aluminum to brass friction stir welding parameters. *Mater. Des.* **2013**, *52*, 587–592.
27. Boldsaikhan, E.; Corwin, E.M.; Logar, A.M.; Arbegast, W.J. The use of neural network and discrete Fourier transform for real-time evaluation of friction stir welding. *Appl. Soft Comput.* **2011**, *11*, 4839–4846.
28. Msomi, V.; Mbana, N.; Mabuwa, S. Microstructural analysis of the friction stir welded 1050-H14 and 5083-H111 aluminium alloys. *Mater. Today Proc.* **2020**, *26*, 189–192.
29. Nakowong, K.; Sillapasa, K. Optimized Parameter for Butt Joint in Friction Stir Welding of Semi-Solid Aluminum Alloy 5083 Using Taguchi Technique. *J. Manuf. Mater. Process.* **2021**, *5*, 88.
30. Cheng, Y.-W.; Read, D.T.; McColskey, J.D.; Wright, J.E. A tensile-testing technique for micrometer-sized free-standing thin films. *Thin Solid Film.* **2005**, *484*, 426–432.
31. Aamir, M.; Tolouei-Rad, M.; Giasin, K.; Vafadar, A. Feasibility of tool configuration and the effect of tool material, and tool geometry in multi-hole simultaneous drilling of Al2024. *Int. J. Adv. Manuf. Technol.* **2020**, *111*, 861–879.
32. Rambabu, G.; Naik, D.B.; Rao, C.V.; Rao, K.S.; Reddy, G.M. Optimization of friction stir welding parameters for improved corrosion resistance of AA2219 aluminum alloy joints. *Def. Technol.* **2015**, *11*, 330–337.
33. Krishnaiah, K.; Shahabudeen, P. *Applied Design of Experiments and Taguchi Methods*; PHI Learning Pvt. Ltd.: Dehli, India, 2012.
34. Ali, M.H.; Wadallah, H.M.; Ibrahim, M.A.; Alomar, O.A. Improving the Microstructure and Mechanical Properties of Aluminium Alloys Joints by Adding SiC Particles During Friction Stir Welding Process. *Metallogr. Microstruct. Anal.* **2021**, *10*, 302–313. https://doi.org/10.1007/s13632-021-00743-9.
35. Cavaliere, P.; Panella, F. Effect of tool position on the fatigue properties of dissimilar 2024-7075 sheets joined by friction stir welding. *J. Mater. Process. Technol.* **2008**, *206*, 249–255.
36. Koilraj, M.; Sundareswaran, V.; Vijayan, S.; Rao, S.K. Friction stir welding of dissimilar aluminum alloys AA2219 to AA5083–Optimization of process parameters using Taguchi technique. *Mater. Des.* **2012**, *42*, 1–7.
37. Sato, Y.S.; Urata, M.; Kokawa, H.; Ikeda, K. Hall–Petch relationship in friction stir welds of equal channel angular-pressed aluminium alloys. *Mater. Sci. Eng. A* **2003**, *354*, 298–305.
38. Yong-Jai, K.; Seong-Beom, S.; Dong-Hwan, P. Friction stir welding of 5052 aluminum alloy plates. *Trans. Nonferrous Met. Soc. China* **2009**, *19*, s23–s27.